# Ultra High-Resolution Imaging using Spatiotemporal Quadratic Phase Encoding

Noam Ben-Eliezer[1], Lucio Frydman[2], and Daniel K Sodickson[1]

[1]*Center for Biomedical Imaging, New-York University Medical Center, New-York, NY, United States,* [2]*Chemical Physics, Weizmann Institute of Science, Rehovot, Israel*

**Background** Imaging at very high resolutions is a challenging task owing to the requirement for high SNR, relatively long echo times and the effect of micro- and macroscopic field inhomogeneities. Another limiting factor is the usually large field-of-views (FOV) that are required in order to avoid aliasing artifacts within the actual region of interest. A recently introduced approach, termed spatiotemporal-encoding (**SPEN**), might hold prospective solutions to these limitations and provide a more optimal approach for imaging at very high resolutions. The approach is based on a temporally progressive refocusing of the image spatial, rather than frequency (*k*-space) domain, using quadratic phase functions [1]. Previous studies have established SPEN's distinct features, including the lack of aliasing / ghosting artifacts, and a unique ability to implement a time- and space-dependent Spin-Echo which fully refocuses all static $T_2^*$ effects for each and every time point –and not just at a single instant as in *k*-domain acquisitions [2-3]. This work presents preliminary results, attesting to SPEN potential for extending the resolution capabilities of MR imaging.

**Methods** Experiments were performed on a 7T whole body Siemens scanner. 2D Spin-Echo (**SE**) sequences based on *k*-space encoding, and on SPEN, were used to image an ultra high-resolution phantom immersed in 2% agar gel, containing an 18mm air filled tube, and a matrix of 0.4mm air and water filled micro-tubes. Quadratic phase-encoding was implemented in the SPEN sequence using a frequency-swept excitation pulse, and then processed using the super-resolved SPEN reconstruction algorithm presented in [5]. Imaging parameters were [*k*-encoded SE: TR/TE=400/11ms, FOV=110x55 mm$^2$, matrix size=512x256, in-plane res=215x215 μm$^2$, slice-thickness=1.5mm]; [SPEN SE: TR/TE=400/(5…20)ms, FOV=55x55 mm$^2$ , matrix size=512x256, in-plane res=108x215 μm$^2$, slice-thickness=1.5mm].

**Results**

The attached Figure shows the resulting images. Left: fully *k*-space encoded images. Right: SPEN, combined with conventional phase-encoding implemented along vertical and horizontal axes respectively. (**a**) Picture of the imaged phantom (top view) prior to immersing it in agar gel. (**b-c**) Full FOV image. Dark regions correspond to 4 Teflon screws, and to the center air-filled tube. (**d-e**) Zoomed view of a 10x10 mm$^2$ ROI covering 4 of the micro-tubes (dashed blue square in (a)). Higher spatial resolution is observed in the SPEN-based image in (d). (**f-g**) Zoomed view of a 10x10 mm$^2$ ROI located in the center of the air-filled tube (dotted white square in (a)). With the grayscale reduced to the image noise level, significantly lower aliasing artifacts are observed for the SPEN image in (g).

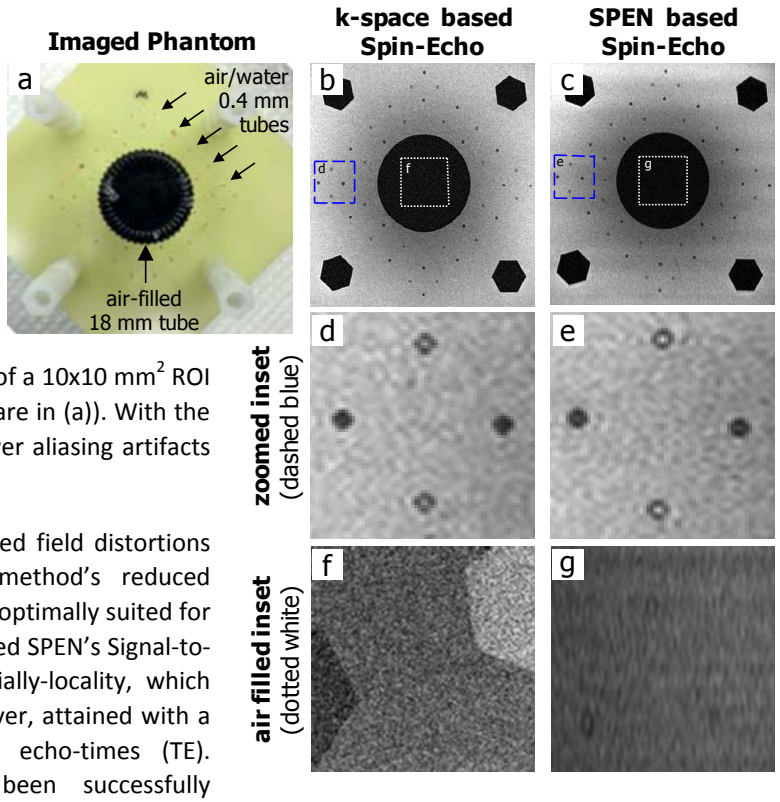


**Discussion** SPEN's unique ability to overcome the increased field distortions characterizing high-field scanners, together with this method's reduced sensitivity to aliasing artifacts, suggest that it might be more optimally suited for high resolution imaging. A recent study has moreover affirmed SPEN's Signal-to-Noise (SNR) comparability to *k*-space imaging. The spatially-locality, which stands at the basis of much of SPEN's advantages, is, however, attained with a cost of either spatially-dependent, or longer minimal echo-times (TE). Notwithstanding, *in-vivo* application of SPEN have been successfully implemented on both human and mouse model, and confirmed its advantage over existing methods in applications involving unfavorable conditions such as those arising in air-filled cavities of the brain, and near metallic implants [6-7].

**References** **[1]** Shrot Y and Frydman L, 2005, *J Magn Res*, v. 172, p. 179-190. **[2]** Chamberlain R et al., 2007, *Magn Res Med*, v. 58, p. 794-799. **[3]** Ben-Eliezer N, Shrot Y and Frydman L, 2010, *Magn Reson Imag*, v. 28(1), p. 77-86. **[4]** Tal A, Frydman L, 2007, *J Magn Res*, v. 189, p. 46-58. **[5]** Ben-Eliezer N, Irani M, Frydman L, 2010, *Magn Reson Med*, v. 63, p. 1594-1600. **[6]** Airaksinen AM et al., 2010, *Magn Res Med*, v. 64, p. 1191-1199. **[7]** Goerke U, Garwood M, Ugurbil K, 2011, *NeuroImage*, v. 54, p. 350-360.

Financial support: ERC Advanced Grant #246754; a Helen Kimmel Award for Innovative Investigation.